# Navier-Stokes Computations and Experimental Comparisons for Rudder Efficiency Analysis in the Moderately Steep Spin Part II: Computation Method

Mirko Kozić, PhD (Eng)[1]

An analysis of the rudder efficiency at flow conditions that correspond to a moderately steep spin is made using a Navier-Stokes code and wind tunnel flow visualization. The code is used for determining the flow field around the LASTA-95 airplane wind tunnel model. The numerical and experimental value of the aerodynamic coefficients and the vector flow field over the vertical tail are compared for configurations with and without the horizontal tail. The purpose of the analysis is in showing the influence of the horizontal tail on the flow field over the vertical tail, especially over the rudder. It is seen that the horizontal tail wake influences the most part of the rudder making it completely inefficient in the spin recovery.

*Key words*: airplane, spinning maneuver, airplane rudder, fluid dynamics, flow visualization, Navier-Strokes equations, effectiveness analysis.

## Introduction

THE spinning maneuver is an uncontrolled rotation of the airplane. It is characterized by the mean wing angle of attack greater than the stalling, approximately vertical velocity of the center of gravity, and a high rate of rotation about the vertical. Empirical methods have been devised [1] [2] [3] [4], in order to help in designing good spin and recovery characteristics for an airplane, or for predicting the spin and recovery characteristics of a specific design. These methods mostly deal with geometric design and the mutual position of the horizontal and vertical tail surfaces.

Because of the fact that steep spinning airplanes recover satisfactorily, while flat spinning airplanes are usually difficult or impossible to recover, one must pay special attention to design parameters that lead to desirable steep spin attitudes. These are: forward location of the center of gravity, high directional stability, large fin area ahead of a line drawn upward and aft 60 degrees from the leading edge of the stabilizer root chord, ventral or dorsal fins, oval shaped aft fuselage cross-section and fin area below horizontal tail [5]. The position of the horizontal tail relative to the rudder has influence on the aerodynamic moment of the rudder, the incidence of the spin and ease of recovery from the spin. The position is recognized as the most important design parameter due to a large shielding effect that can change completely the effectiveness of the rudder.

The shielding effect of the horizontal tail can be obtained by means of the wind-tunnel testing or computational fluid dynamics (CFD) codes. CFD simulations only approximate the complex flow phenomenon, so that even with meshes containing 100 million of cells, all answers will not be obtained. The CFD simulations play an important role in eliminating preliminary models at the beginning of the design process and leaving expensive wind tunnel testing for detailed models that are close to the final design. In this way the quantity of the wind tunnel experiments will be reduced to a great extent.

In the paper CFD is used in obtaining results that are compared to the wind tunnel ones, for incidence that is related to moderately steep spin. Besides aerodynamic coefficients, also the velocity field over the vertical stabilizer and rudder is also compared for two configurations, with and without the horizontal tail.

## Computational method

The code used in this study employs a cell-centered finite volume method based on the linear reconstruction-evolution method of Anderson-Tomas-Van Leer (TVD/MUSCL) [7] [8]. Diffusion terms are discretized by central differences. The discretized algebraic equations are solved using point-wise Gauss-Seidel iterative algorithm.

The reconstruction-evolution methods have a strong physical background. They consist of two steps, spatial reconstruction and temporal evolution. In the first step the exact solution is reconstructed inside each cell of the numerical domain using the numerical values from the previous time step. This step need not account for the upwind direction, and may involve solution averaging and slope limiting, i.e. the elements that characterize solution sensitive methods. In the second step the reconstructed solution is developed from time the level n to $n+1$ using characteristics or some other technique, in order to obtain the time averaged numerical flux at the boundary of each cell.

These methods are sometimes called Godunov-type methods, after such first-order method, especially when the time developing uses the exact Riemann solver.

The Anderson-Tomas-Van Leer method is a conservative semi discrete method. Applied to the nonlinear one-dimensional scalar conservation law

[1] Military Technical Institute (VTI), Ratka Resanovića 1, 11132 Belgrade, SERBIA

$$\frac{\partial u}{\partial t} + \frac{\partial f(u)}{\partial x} = 0 \qquad (1)$$

where $u$ is a conservative variable and $f$ is flux function, it can be written as

$$\frac{d\overline{u}_i^n}{dt} + \frac{\hat{f}_{s,i+\frac{1}{2}}^n - \hat{f}_{s,i-\frac{1}{2}}^n}{\Delta x} = 0 \qquad (2)$$

where $\overline{u}_i^n$ is approximately an average of the exact value of the conservative variable in a cell $i$ at a time level $n$

$$\overline{u}_i^n \approx \frac{1}{\Delta x} \int_{x_{i-\frac{1}{2}}}^{x_{i+\frac{1}{2}}} u\left(x, t^n\right) dx \qquad (3)$$

The semi discrete conservative numerical flux at the edge of the cell $i$ is simply

$$\hat{f}_{s,i+\frac{1}{2}}^n \approx f\left(u\left(x_{i+\frac{1}{2}}, t^n\right)\right) \qquad (4)$$

Splitting the flux in two parts that correspond to the left and right-running waves as

$$f(u) = f^+(u) + f^-(u) \qquad (5)$$

the semi discrete flux can be written as

$$\hat{f}_{s,i+\frac{1}{2}}^n \approx f^+\left(u\left(x_{i+\frac{1}{2}}, t^n\right)\right) + f^-\left(u\left(x_{i+\frac{1}{2}}, t^n\right)\right) \qquad (6)$$

The part of the flux that takes into account the right-running wave i.e. $f^+\left(u\left(x_{i+\frac{1}{2}}, t^n\right)\right)$ is approximated with a leftward bias using reconstruction from the cell-integral averages, or so called reconstruction via the primitive function. The part of the flux that corresponds to the left-running wave, i.e. $f^-\left(u\left(x_{i+\frac{1}{2}}, t^n\right)\right)$ is approximated with a rightward bias.

The second-order accurate linear reconstruction via the primitive function using the leftward bias yields

$$u(x, t^n) \approx \overline{u}_i^n + \frac{\overline{u}_i^n - \overline{u}_{i-1}^n}{\Delta x}(x - x_i) \qquad (7)$$

At the edge of the cell $i$ it gives

$$u\left(x_{i+\frac{1}{2}}, t^n\right) \approx \overline{u}_i^n + \frac{1}{2}(\overline{u}_i^n - \overline{u}_{i-1}^n) \qquad (8)$$

The first order accurate constant reconstruction at the edge of the cell $i$ with the leftward bias is

$$u\left(x_{i+\frac{1}{2}}, t^n\right) \approx \overline{u}_i^n \qquad (9)$$

Instead of using pure linear or pure constant reconstruction, the Anderson-Tomas-Van Leer method uses the convex linear combination,

$$u_{i+\frac{1}{2}}^+ = \overline{u}_i^n + \frac{1}{2}\phi_i^+(\overline{u}_i^n - \overline{u}_{i-1}^n) \qquad (10)$$

where $\phi_i^+$ is the adaptive parameter controlling the linear combination, i.e. the parts of linear and constant reconstruction in the linear combination. It is called a slope limiter. It is chosen to ensure nonlinear stability.

The similar procedure is done for the rightward bias, and finally the semi discrete flux is given as

$$\hat{f}_{s,i+\frac{1}{2}}^n = f^+\left(u_{i+\frac{1}{2}}^+\right) + f^-\left(u_{i+\frac{1}{2}}^-\right) \qquad (11)$$

or explicitly

$$\hat{f}_{s,i+\frac{1}{2}}^n = f^+\left(\overline{u}_i^n + \frac{1}{2}\phi_i^+(\overline{u}_i^n - \overline{u}_{i-1}^n)\right) + \\ + f^-\left(\overline{u}_{i+1}^n - \frac{1}{2}\phi_{i+1}^-(\overline{u}_{i+2}^n - \overline{u}_{i+1}^n)\right) \qquad (12)$$

Two approaches can be used in treating turbulence. The first one is based on the time averaged Navier-Stokes equations and different turbulence models that close the system of partial differential equations describing conservation laws. These include $k\text{-}\varepsilon$, $k\text{-}\omega$, Spalart-Allmaras and Reynolds stress model.

The second approach is a large-eddy-simulation in which large eddies are computed because they are directly affected by the boundary conditions, whereas the smallest eddies are modeled for their universal characteristics and nearly isotropic properties. Filtering must be used in deriving the resolvable-scale equations.

## Results

The comparison between the computed results and the experimental data is presented for two configurations, with and without the horizontal tail. The main intention is to show the shielding effect of the horizontal tail on the rudder at the fixed incidence equal to 44.47°, that corresponds to a moderately steep spin, and is characterized with massive separation from the whole configuration.

In the CFD analysis the wind tunnel model is considered. In this way both the influence of the tunnel walls is taken into account and the true value of turbulence intensity ahead of the model. But it introduced an additional difficulty, because for each configuration at each sideslip angle, new mesh had to be generated. Due to very complex geometry of the model unstructured meshes were used. Each mesh consists of about 840000 cells, and this number is dictated only by computer resources. The Spalart-Allmaras turbulence model [9] is used, in which a partial differential equation for transport of turbulent viscosity is separately solved from the flow equations. Two reasons influenced this choice. First, it is well suited for aeronautical problems with an adverse pressure gradient, and second it does not use the wall functions, which lose any justification in the situation with massive separation.

The best choice would be the large eddies simulation, but the mesh is too crude and only eddies the size of which is of the order or larger than the smallest cell size, can be resolved, whereas smaller ones have to be modeled.

The first set of results corresponding to the drag and lift coefficient is given in Table 1.

The experimental values are given in [10], and it can be seen that the largest differences between the numerical and the experimental values are 5.2% and 6.9% for the drag and the lift coefficient respectively. The agreement is quite good keeping in mind that the configurations are rather complex and the meshes are relatively crude. This can be explained by the fact that at the considered incidence the position of the separation point is fixed at the leading edge of the lifting surface and there is no reattachment. Otherwise, at the angles of attack around the stall, the

character of separation and reattachment is much more complex, thus strongly influencing the values of the aerodynamics coefficients and the lift curve character.

**Table 1.**

| configuration & flow conditions: angle of attack sideslip angle freestream velocity | drag coefficient $C_x$ | | lift coefficient $C_z$ | |
|---|---|---|---|---|
| | experimental | numerical | experimental | numerical |
| wing-fuselage-vertical tail horizontal tail $\alpha = 44.47^o$ $\beta = 0^o$ $V = 38$ m/s | 0.9941 | 1.0131 | 1.05 | 1.06 |
| wing-fuselage-vertical tail –horizontal tail $\alpha = 44.47^o$ $\beta = -10^o$ $V = 35$ m/s | 0.9723 | 1.0257 | 1.01 | 1.08 |
| wing-fuselage vertical tail $\alpha = 44.47^o$ $\beta = 0^o$ $V = 35$ m/s | 0.8665 | 0.8961 | 0.90 | 0.94 |
| wing-fuselage-vertical tail $\alpha = 44.47^o$ $\beta = -10^o$ $V = 35$ m/s | 0.8736 | 0.8880 | 0.91 | 0.94 |

In Fig.1 the relative static pressure distribution over the airplane surface is shown for the wing-fuselage-vertical tail-horizontal tail configuration. It can be noticed that the pressure distribution is asymmetrical due to the sideslip angle.
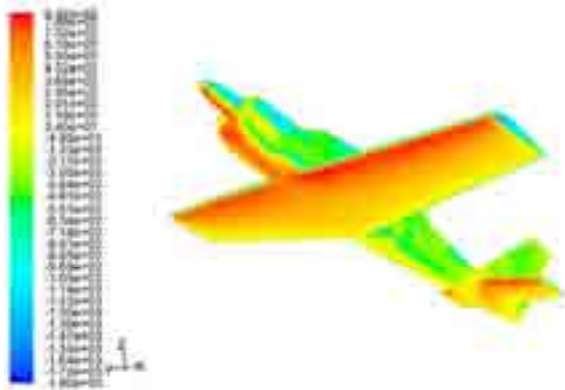


**Figure1.** Relative static pressure distribution over the surface of the wing-fuselage-vertical tail -horizontal tail configuration at flow conditions $\alpha = 44.47^o$, $\beta = -10^o$, $V = 35$ m/s.

The second set of the results gives the velocity vector field over the vertical stabilizer and the rudder.



**Figure 2.** Numerical velocity vector field over the vertical tail for the wing-fuselage-vertical tail-horizontal tail configuration and the flow conditions: angle of attack $\alpha = 44.47^o$, sideslip angle $\beta = 0^o$, free-stream velocity $V = 38$ m/s



**Figure 2a.** Experimental velocity vector field over the leeward side of the vertical tail for the wing-fuselage-vertical tail-horizontal tail configuration and the flow conditions: angle of attack $\alpha = 44.47^o$, sideslip angle $\beta = -10^o$, free-stream velocity $V = 35$ m/s
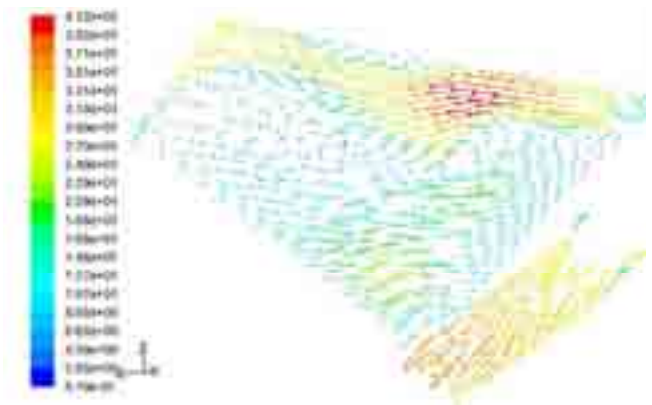


**Figure 2b.** Velocity vector field over the leeward side of the vertical tail for the wing-fuselage-vertical tail-horizontal tail configuration and the flow conditions: angle of attack $\alpha = 44.47^o$, sideslip angle $\beta = -10^o$, free-stream velocity $V = 35$ m/s



**Figure 3a.** Experimental velocity vector field over the vertical tail for the wing-fuselage-vertical tail configuration and the flow conditions: angle of attack $\alpha = 44.47^o$, sideslip angle $\beta = 0^o$, free-stream velocity $V = 35$ m/s

**Figure 3b.** Velocity vector field over the vertical tail for the wing-fuselage-vertical tail-horizontal tail configuration and the flow conditions: angle of attack $\alpha = 44.47^o$, sideslip angle $\beta = 0^o$, free-stream velocity $V = 35$ m/s



**Figure 4a.** Experimental velocity vector field over the leeward side of the vertical tail for the wing- fuselage-vertical tail configuration and the flow conditions: angle of attack $\alpha = 44.47^o$, sideslip angle $\beta = -10^o$, free-stream velocity $V = 35$ m/s
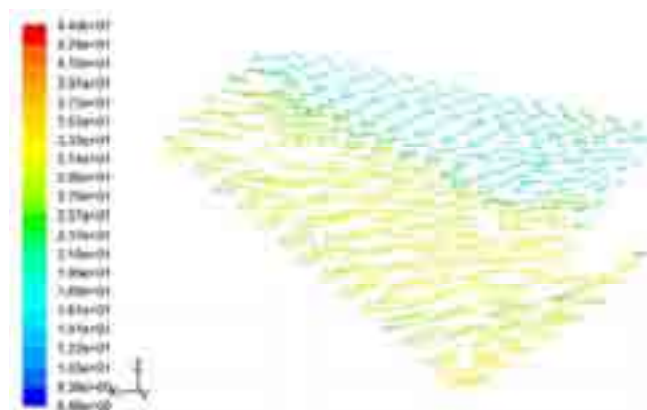


**Figure 4b.** Velocity vector field over the leeward side of the vertical tail for the wing-fuselage-vertical tail-horizontal tail configuration and the flow conditions: angle of attack $\alpha = 44.47^o$, sideslip angle $\beta = -10^o$, free-stream velocity $V = 35$ m/s

Comparing the numerical and the experimental velocity vector field over the vertical tail, for the configurations with and without the horizontal tail, it is obvious that the eddies generated in the separated wake of the horizontal tail, pass over the rudder making it completely ineffective. In the configurations with the horizontal tail, only a small portion of the clean flow exists over the rudder, i.e. the portion below the horizontal tail as seen in Figures 1 and 2b. The numerically and experimentaly obtained velocity vector fields over the vertical tail are in a good qualitative agreement.

## Conclusion

A three-dimensional unstructured Navier-Stokes code has been utilized for computing and analyzing the flow field around the wind tunnel model of the LASTA-95 airplane with and without the horizontal tail under the conditions that correspond to a moderately steep spin. The comparisons between the computed and the experimental aerodynamic coefficients and the velocity field over the vertical stabilizer and the rudder are made for the angle of attack equal to $44.47^o$. The influence of the horizontal tail wake on the velocity field over the rudder is clearly shown.

The effectiveness of the rudder practically disappears, due to the shielding effect of the horizontal tail.

This example shows the usefulness of CFD, that should be used in the beginning stages of a design, in which such problems could be recognized and solved thus preventing their appearance in the final design.

## References

[1] PAMADI,B.N., TAYLOR,JR.,L.W.: *Estimation of Aerodynamic Forces and Moments on a Steadily Spinning Airplane*, Journal of Aircraft, 1984,Vol.21, No.12, pp.943-954

[2] BIHRLE,W.Jr., BARNHART,B., PANTASON,P.: *Static Aerodynamic Characteristics of a Typical Single Engine Low Wing General Aviation Design for an angle of Attack Range – 8 Degrees to 90 Degrees*, NASA CR-2971, 1978.

[3] BEAURAIN,L.: *General Study of Light Plane Spin*, Aft Fuselage Geometry, Part I, NASA TTF-17446,1977.

[4] BIHRLE,W.Jr., BOWMAN,J.S.Jr.: *Influence of Wing*, Fuselage and Tail Design on Rotational Flow Aerodynamics Beyond Maximum Lift, Journal of Aircraft, Vol.18, Nov. 1981, pp.920-930.

[5] KERR,T.H., SHORR,M.: *Spinning, Agard Flight Test Manual*, Volume II, Chapter 8

[6] KOZIĆ,M.: *Comparison of the Navier-Stokes Computations with experiment for LASTA-95 wing at high angles of attack*, Scientific Technical Review, 2006, Vol.LVI, No.1, pp.41-44.

[7] ANDERSON,W.K., THOMAS,L.L., VAN LEER,B.: *Comparison of Finite Volume Flux Vector Splitting for the Euler Equations*, AIAA Journal, No.24, pp.1453-1460, 1986.

[8] LANEY,C.: *Computational Gasdynamics*, Cambridge University Press, 1999.

[9] SPALART,P.R., ALLMARAS,S.R.: *A one equation turbulence model for aerodynamic flows*, La Recherche Aerospatiale, No.1, 1994, pp.5-21.

[10] OCOKOLJIĆ,G., ANASTASIJEVIĆ,Z.: *Determination of aerodynamic coefficients and visualization of the flow around the LASTA-95 aircraft model, Part I: Experimental Method*, Scientific Technical Review, 2008, Vol.LVIII, No.1, pp.55-60.

# Izračunavanja Navije-Stoksovim jednačinama i poređenja sa eksperimentom u analizi efikasnosti krmila pravca u umereno strmom kovitu

Koristeći Navijer-Stoks-ov softver i vizualizaciju strujanja u aerotunelu, izvršena je analiza efikasnosti krmila pravca za uslove strujanja koji odgovaraju umereno strmom kovitu. Ovim softverom određeno je strujno polje oko aerotunelskog modela aviona LASTA-95. Porede se numeričke i eksperimentalne vrednosti aerodinamičkih koeficijenata i polje vektora brzine oko vertikalnog repa za konfiguracije sa i bez horizontalnog repa. Cilj analize je da se pokaže uticaj horizontalnog repa na strujno polje na vertikalnom repu, posebno na krmilu pravca. Vidi se da vrtložni trag horizontalnog repa utiče na najveći deo krmila pravca, čineći ga potpuno neefikasnim u vađenju iz kovita.

*Ključne reči*: avion, kovit, avionsko krmilo, dinamika fluida, vizuelizacija strujanja, Navije-Stoksove jednačine, analiza efikasnosti.

# Вычисления уравнениями Навиер-Стокса и сравнивания с экспериментом в анализе эффективности руля направления в умеренно крутом штопоре

Пользуя программное обеспечение Навиер-Стокса и визуализацию потока в аэродинамической трубе, в настоящей работе проведен анализ эффективности руля направления для условий потока, соответствующих умеренно крутом штопору. Этим программным обеспечением определено поле потока около модели самолета «Ласточка-95» в аэродинамической трубе. Здесь сравниваются численные и экспериментальные значения аэродинамических коеффициентов и поле вектора скорости около вертикального хвостового оперения для конфигураций со и без горизонтального хвостового оперения. Цель анализа – показать влияние горизонтального хвостового оперения на поле потока на вертикальном хвостовом оперении, а особенно на руле направления. Тогда видно, что спустная струя за горизонтальным хвостовым оперением влияет на наибольшую часть руля направления, делая его совсем неэффективным при выводе из штопора.

*Ключевые слова*: самолет, штопор, бортовой руль, динамика жидкостей, визуализация потока, уравнения Навиер-Стокса, анализ эффективности.

# Computations Navier-Stokes et comparaison expérimentale pour l'analyse de l'efficacité du gouvernail dans la vrille modérément raide Deuxième partie: méthode de comparaison

En utilisant le logiciel Navier-Stokes et la visualisation du courant dans la soufflerie aérodynamique on a fait l'analyse de l'efficacité du gouvernail pour les conditions du curant qui correspondent à la vrille modérément raide. Le champ du courant autour du modèle d'avion LASTA-95 a été déterminé par ce logiciel dans la soufflerie aérodynamique. On a comparé les valeurs numériques et expérimentales des coefficients aérodynamiques et le champ du vecteur de la vitesse autour de la queue verticale pour la configuration avec ou sans queue horizontale. Le but de l'analyse était de démontrer l'influence de la queue horizontale au champ de courant sur la queue verticale et surtout au gouvernail. On voit que la trace de la queue horizontale influence sur la grande partie de gouvernail en le rendant complètement inefficace dans le redressement de la vrille.

*Mots clés*: avion, vrille, gouvernail d'avion, dynamique des fluides, visualisation du courant, équations Navier-Stokes, analyse de l'efficacité.